

Melissa S. Bukovsky^{1*} and David J. Karoly²

¹University of Oklahoma, Norman, OK

²University of Melbourne, Melbourne, AUS

1. INTRODUCTION

Precipitation from select GCMs run for the IPCC AR4 is examined in this paper. A suite of twenty-three models was run in support of the AR4 effort. They have horizontal resolutions ranging from 1°-3°, approximately, and most of them no longer use flux adjustment (artificial adjustments to heat, water, and momentum fluxes) to maintain a stable control climate. As stated in the AR4, "[t]here is considerable confidence that climate models provide credible quantitative estimates of future climate change, particularly at continental scales and above" (Randall et al. 2007, pg. 600). This is because models have a physical foundation and the ability to represent current and past climate with reasonable accuracy. However, simulation for certain variables and processes is still better for some than for others.

This paper will explore the simulation of precipitation in five of the models used in the AR4 over the US, focusing on summertime precipitation. As all aspects of this review are problematic for the AR4 suite of models in terms of the size of the region, the variable chosen, and the season of interest in the chosen region, this effort mainly aims to identify the specific inaccuracies over the US and discuss potential reasons for their existence. Therefore, this paper will focus on precipitation from simulations of the 20th century, but we will take a brief look at some aspects from simulations of future climate.

2. MODELS AND METHODS

Precipitation from the following coupled global climate models will be used in this intercomparison: NCAR's Community Climate System Model version 3.0 (CCSM 3.0, Collins et al. 2006); the Geophysical Fluid Dynamics Laboratory (GFDL) climate model version 2.0 (GFDL 2.0, Delworth et al. 2006); the National Aeronautics and Space Administration (NASA) Goddard Institute for Space Studies (GISS) Model EH (Model E with the HYCOM ocean model) (GISS EH, Schmidt et al. 2006); and the Center for Climate System Research (The University of Tokyo), the National Institute for Environmental Studies, and the Frontier Research Center for Global Change's medium and high resolution Model for Interdisciplinary Research on Climate (MIROC-MED

and MIROC-HI, Hasumi and Emori 2004). Output from all models is available from the Program for Climate Model Diagnosis and Intercomparison (PCMDI) in support of the IPCC's 4th assessment. In part, these models were chosen because three or six hourly precipitation data are available from each for overlapping 20th century time periods. Simulations in section 3 use the IPCC 20C3M (20th century) scenario, while those in section 4 where run using the A2 and A1B (future) emission scenarios. Three-hourly values from the GCMs are only available from 1991-2000 (except for the CCSM 3.0 which is only available every 6 hours from 1991-1999); therefore, the 1990s are the chosen decade for the 20th century part of this study. For each emission scenario, multiple runs may be available. However, output with a higher time frequency (3-6h) is usually only offered for one of them. Here, all data are for run one, except for the CCSM 3.0 and GISS EH for which run 5 is used (3h data are not available from the other runs). For the brief examination of future precipitation in section 4, daily climate model output will be used, as 3-6 hourly output is either not obtainable or not available for more than at least a 5 year period for most of the chosen models.

All models will be used at their original horizontal resolution. This gives the greatest impression of how much information can be gleaned from the data, and, furthermore, scaling them to matching grids does not change the overall results. For the 20th century intercomparison presented in section 3, model precipitation will be compared to precipitation from the NARR, as the NARR was found to be the most reliable, highest-resolution, gridded, observation based dataset in terms of precipitation in Bukovsky and Karoly (2007).

2.1 CCSM 3.0

The CCSM 3.0 is a fully coupled global climate model containing atmosphere, ocean, sea ice, and land surface components. It contains a Eulerian spectral dynamical core with a triangular spectral truncation at T85 (approximately 1.4°) and 26 sigma-pressure hybrid vertical layers in the atmosphere with no flux correction (Collins et al. 2006). The resolution of the ocean model is set at 1°. This model utilizes the Zhang and McFarlane (1995) CPS for deep convection only. This CPS is a simplified version of the AS scheme. Convective available potential energy (CAPE) is required for deep convection, and a low-level unstable parcel will convect if it can penetrate any stable layer. A parameterization for shallow and

* Corresponding author address: Melissa S. Bukovsky, School of Meteorology, Univ. of Oklahoma, 120 David L. Boren Blvd., Norman, OK 73072; email: mbukovskv@ou.edu

upper-level convection developed by Hack (1994) is included, and large-scale condensation is treated prognostically, as described in Rasch and Kristjansson (1998) (with modifications by Zhang et al. 2003) (Boville et al. 2006).

2.2 GFDL 2.0

The GFDL 2.0 is also a fully couple global climate model containing atmosphere, ocean, sea ice, and land components. It contains a B-grid dynamic core with 2° latitude by 2.5° longitude resolution and 24 vertical levels in the atmospheric component and no flux adjustments (Delworth et al. 2006). Ocean resolution is 1° with increasing resolution equatorward of 30° to a 1/3° grid spacing. The dynamic core in this version of the GFDL CM is responsible for the equatorward drift of the mid-latitude westerlies over time seen in its simulations. This is eliminated in version 2.1 with the use of a finite volume dynamical core. Precipitation is, however, simulated better in version 2.0 than version 2.1 (Delworth et al. 2006). Convection in GFDL 2.0 is parameterized using the relaxed AS scheme proposed by Moorthi and Suarez (1992). Closure in this version of AS is still based on quasi-equilibrium, except that quasi-equilibrium is not required with the large-scale forcing; it is obtained, approximately, on shorter time scales depending on cloud type. That is, the CPS relaxes the cloud work function for each cloud type to a specified value. Convective downdrafts are not included in this version of the CPS. Large-scale condensation is computed in a prognostic sense using Rotstayn (1997) and Tiedtke (1993).

2.3 GISS EH

The GISS EH model is the coarsest resolution global coupled climate model used in this study at 4° latitude by 5° longitude on an Arakawa B grid with 20 mixed sigma-pressure layers. Convection is based on the mass-flux-type-scheme by DelGenio and Yao (1993) and DelGenio et al. (1996). In this scheme, convection triggers when an air parcel lifted one level saturates and becomes buoyant. Convection transports enough mass for parcels lifted from cloud base to obtain neutral buoyancy. Downdrafts are allowed for parcels that rise more than one level. Large scale condensation is prognostic and based on moisture convergence (Sundqvist 1978, Sundqvist et al. 1989).

2.4 MIROC-HI AND MIROC-MED

The two MIROC models examined here differ only in resolution. They are both global coupled models with five components: atmosphere, land, river, sea ice, and ocean. MIROC is a spectral model and uses a sigma coordinate system in the vertical.

MIROC-HI has a spectral truncation of T106 (~1.125°) and 56 vertical layers while MIROC-MED has a truncation of T42 (~2.8125°) and 20 vertical layers. The convective parameterization is a simplified version of AS where the closure has been changed from a diagnostic quasi-equilibrium closure to a prognostic cumulus kinetic energy closure based on Pan and Randall (1998). In addition, cumulus convection is not allowed when the cloud-mean ambient relative humidity is less than 80%. Downdrafts are included in this CPS. Large-scale condensation is based on Le Treut and Li (1991).

2.5 Future Scenarios

Future climate change results are based on emission scenarios developed by the IPCC. Predicting concentrations of greenhouse gases is obviously subject to considerable uncertainty given the many difficult to predict factors that may control them. Therefore, a number of possible scenarios were developed for use by the IPCC (IPCC 2000). They outline emissions of carbon dioxide, methane, nitrous oxide and sulfur dioxide. The IPCC A2 and A1B were chosen for the future simulations used in section 4 because they represent high and mid-range emissions and because model output is available. The A2 scenario is based on a very heterogeneous world, where the population is continuously increasing, economic development is regionally oriented, and technological change and economic per capita growth is fragmented and relatively slow. The A1B scenario describes a more homogeneous world with a population that peaks in mid-century and then declines. New, more efficient technologies evolve more rapidly, and the use of fossil fuels and alternative energy sources is balanced (IPCC 2000).

3. RESULTS: PRESENT CLIMATE

As illustrated in Fig. 1 the only feature in the distribution of the annual average precipitation over the US that is captured throughout the suite of models examined here is the maximum in precipitation over the Pacific Northwest, the maximum in the Southeast is not consistently represented. For instance, GFDL 2.0 is generally too wet over the eastern half of the US, except over Florida where it is too dry. The CCSM 3.0 does not have a Southeast maximum and produces a plethora of precipitation over the Gulf Stream like some of the other models. MIROC-MED and MIROC-HI highlight most of the east coast with the exception of the MS, AL, GA, and FL region. The best distribution of the annual average precipitation seems to be produced by the lowest resolution model, GISS EH, but the intensity of the precipitation is so light that the values plotted in Fig. 1c had to be multiplied by a factor of four so that some detail could be seen using the chosen contour values.

The annual cycle of precipitation over the US is roughly captured by most of the climate models (right half of Fig. 1). Over the eastern half of the country, the peak in precipitation rate occurs in the summer, except in MIROC-MED and MIROC-HI, which produce an extraordinary amount of precipitation over the Gulf Stream around October. The general seasonal and diurnal distribution of precipitation over the western half of the US is superior to that over the eastern half. The diurnal spread is greatest in the summer with dominant afternoon/evening precipitation, and cool season precipitation is greater than warm season due to the NW maximum. The greatest problem over the western half of the nation is in the magnitude of the precipitation rate.

The simulation of the predominantly convective JJA precipitation is not highly improved over the annual average, as expected. Fig. 2 shows the time and magnitude of the maximum precipitation for the various models. All but MIROC-MED capture the summertime maximum over the southeast US. The distribution seems to be best in the GISS-EH, except over FL, where important land-sea interactions are likely not well resolved. The CCSM 3.0 and MIROC-HI have the most accurate time for the maximum precipitation in the Southeast.

The summertime Great Plains nocturnal maximum is not particularly well captured in any model. The GFDL 2.0 and MIROC-MED do simulate an early afternoon maximum that appears to be orographically forced, and MIROC-HI produces a late afternoon maximum in Colorado, but no model seems to propagate this precipitation into the Plains. The GISS-EH produces a decent distribution, considering its resolution, but the maximum occurs around noon local solar time (LST), approximately twelve hours early. The Great Plains maximum and timing is best represented by the CCSM 3.0. Precipitation is not intense enough into IA, MN, and WI, but the timing of the maximum on the CO front range is only off by about 3h and there is some extension of that precipitation into the central Plains; although, given the time vectors (and Hovmöller diagrams, not shown), this does not appear to be precipitation propagating off the front range.

The frequency distribution of precipitation rates greater than 5 mm/day for the central US is shown in Fig. 3 (the region in question is outlined in Fig. 2a). Frequency is defined as the percentage of days per 3h period at any point in the region with a given precipitation rate out of all possible days and points with data. Examining precipitation above the 5 mm/day value excludes some of the lighter precipitation rates that are too frequent in the climate models, even in this newest generation of models (Sun et al. 2006). Fig. 3d shows that the GISS-EH produces precipitation that is too light too frequently (although at this resolution it is expected to be lighter,

here the original precipitation rates have been multiplied by a factor of 3). The GFDL 2.0 also precipitates too frequently in the 5-55 mm/day category, while the two MIROC models produce values that are much closer to what is observed. The most frequent precipitation in the 5-55 mm/day category occurs roughly between 1800 and 0000 UTC in all of the models, which is close to observed. Precipitation rates greater than 55 mm/day does not occur frequently enough in any model except MIROC-HI, which has the most representative frequency distribution, even though the diurnal cycle is off. The CCSM 3.0, although one of the higher resolution models, does not produce enough intense precipitation in this portion of the country (that this is from 6h and not 3h average precipitation does not make a difference, not shown), it produces a distribution close to that of the MIROC-MED only with a much-amplified diurnal cycle. As far as being able to produce precipitation rates greater 155 mm/day, the GFDL 2.0, is probably the second best in that it does produce precipitation in this range with any frequency greater than zero, although the greatest frequency occurs about 3-6 hours late.

The percentage of extreme precipitation from the total precipitation in any given model in JJA is better than the magnitude of the extreme precipitation in the frequency distribution (fig. 4). About 4-12% of the total precipitation east of the Continental Divide is from precipitation events heavier than the 90th percentile, and this is generally captured by all models. This does not include the SE or Great Plains nocturnal maximum, however, as the distribution in Fig. 2 is echoed here.

4. RESULTS: FUTURE CLIMATE

Results from future simulations of precipitation are subject to the same distribution problems shown above and, thus, must be used with caution over any given region in the US. General trends and variation between models, however, may provide useful insight into the future of precipitation over the US. Two statistics will be briefly examined here for two climate change scenarios. The models from the previous section that have data available will be used.

The percent change in annual mean precipitation rate between the 1990's and 2081-2100 are given in Fig. 5. Three of the four models agree that there will be a decrease in annual mean precipitation over the central US by the end of the 21st century of about 10-20% depending on the model, scenario, and location. The outlier, the CCSM 3.0, predicts an increase in annual mean precipitation for this region. A decrease is predicted throughout all simulations for the SW US. These trends are echoed in JJA precipitation (not shown), but to a greater extent. The only regions predicted in all models and

scenarios to see an increase in annual mean precipitation is the far NE and WA state.

While a decrease in mean annual and JJA (not shown) precipitation in the central US is predicted by three of the models, an increase in heavy JJA precipitation is expected in the same three models (fig. 6). Once again, the CCSM 3.0 is in opposition. In most cases, the magnitude of any change here and in average precipitation is greater in the SRESA2 scenario than in the SRESA1B scenario, as anticipated given the greenhouse gas concentration over time in each scenario.

5. DISCUSSION

The results presented in section 3 agree with results presented in other studies. For instance, Sun et al. (2006) show that frequency of light precipitation is overestimated and the frequency of heavy precipitation is under estimated by current GCMs, as is seen here in most cases. The higher resolution models examined above tend to exhibit better spatial patterns of precipitation, with the exception of the GISS-EH which is the coarsest resolution model, yet still does fairly well with distribution (not intensity). The MIROC-HI also shows an improved solution for the intensity and frequency of intense precipitation. These agree with the results presented by Duffy et al. (2003) using the Community Climate Model 3 (CCM3); wherein, the increase in resolution from T42 to T170 to T239 led to an improved spatial distribution and intensity of extreme precipitation over the US. The same study also showed that the JJA nocturnal precipitation maximum in the center of the country did not improve with resolution changes only and stated that the same misplaced maximum occurs in most CMIP (Coupled Model Intercomparison Project) models.

The diurnal cycle and frequency of precipitation is also highly related to convective parameterization; the CPS used, therefore, is of great importance in the warm season when most CONUS convection occurs (Heideman and Fritsch 1988). Triggering and closure methods dictate when and where convection will occur. As mentioned, JJA convection in the Southeast is related to surface heating and atmospheric instability. It is not surprising, therefore, that most of the models discussed above captured the maximum in precipitation and its timing in this part of the country fairly well as all but the GISS-EH use CAPE-based triggers (i.e. CAPE greater than zero with possibly one other constraint triggers convection). The maximum over FL may not be captured well, but this may be a resolution issue and less related to physical parameterizations (i.e. FL may not be a well resolved land mass).

Problems in the representation of precipitation in the central US were expected in all of

the climate models as the propagation of convective systems and, specifically, the nocturnal precipitation maximum are major modeling problems (Davis et al. 2003). Convective inhibition usually allows instability to build up before intense convection triggers. Triggering is also linked to large-scale forcing in this region. Furthermore, all but the GISS-EH use triggers that do not use parcel theory and instead rely on the existence of CAPE. Therefore, the frequent triggering of weaker convection is expected (Xie et al. 2002). Some of the models appear to initiate convection just east of the Rockies, but all are too early (they peak more with the daytime heating cycle) except one. The CCSM 3.0 maximizes convection at a more realistic time, but fails to propagate it. For convection to propagate its effects must be felt on the grid-scale through upscale growth which is problematic in mesoscale models and probably not possible in climate models at the resolution they are currently being run. The more realistic initiation time may be a result of the added constraint in the CCSM 3.0 CPS trigger that a parcel must be able to rise through a stable layer to convect; thus, accounting for the presence of convective inhibition (CIN) to some extent.

6. CONCLUDING REMARKS

The main purpose of this comparison was to document the extent to which some regional precipitation characteristics can be represented in climate models. The results agree well with other studies in that warm season precipitation in climate models tends to be too early, too frequent, and not intense enough. Increased resolution holds some promise for improving the representation of precipitation, but physical parameterizations do not always perform as expected as resolution is increased, which complicates the issue (Duffy et al. 2003). Choice of convective parameterization can have a big impact on precipitation simulation, but most of the models examined here used a similar type of convective scheme and, thus, gave similar results. As climate prediction of precipitation is important for forecasting local and regional impacts of future climate change and often for seasonal to interannual prediction, it is valuable to document model simulation characteristics and diagnose problems as the first step towards improving them.

Acknowledgements

The authors acknowledge the international modeling groups for providing their data for analysis, the Program for Climate Model Diagnosis and Intercomparison (PCMDI) for collecting and archiving the model data, the JSC/CLIVAR Working Group on Coupled Modeling (WGCM) and their Coupled Model Intercomparison Project (CMIP) and Climate

Simulation Panel for organizing the model data analysis activity, and the IPCC WG1 TSU for technical support. The IPCC Data Archive at Lawrence Livermore National Laboratory is supported by the Office of Science, U.S. Department of Energy. This work was supported by the Gary Comer Foundation for Science and Education.

REFERENCES

- Boville, B. A., P. J. Rasch, J. J. Hack, and J. R. McCaa, 2006: Representation of clouds and precipitation processes in the Community Atmosphere Model (CAM3). *J. Climate*, **19**, 2184–2198.
- Bukovsky, M. S. and D. J. Karoly, 2007: A brief evaluation of precipitation for the North American Regional Reanalysis. *J. Hydrometeorology*, **8**, 837–846.
- Collins, W. D., C. M. Bitz, M. L. Blackmon, G. B. Bonan, C. S. Bretherton, J. A. Carton, P. Chang, S. C. Doney, J. J. Hack, T. B. Henderson, J. T. Kiehl, W. G. Large, D. S. McKenna, B. D. Santer, and R. D. Smith, 2006: The Community Climate System Model: CCSM3. *J. Climate*, **19**, 2122–2143.
- Davis, C. A., K. W. Manning, R. E. Carbone, S. B. Trier, and J. D. Tuttle, 2003: Coherence of warm-season continental rainfall in numerical weather prediction models. *Mon. Wea. Rev.*, **131**, 2667–2679.
- DelGenio, A. D. and M. S. Yao, 1993: Efficient cumulus parameterization for long-term climate studies: The GISS scheme. *The Representation of Cumulus Convection in Numerical Models*, Emanuel, K. and D. Raymond, Eds., American Meteorological Society, No. 46 in AMS Meteor. Monograph, 181–184.
- DelGenio, A. D., M. S. Yao, W. Kovari, and K. K. Lo, 1996: A prognostic cloud water parameterization for general circulation models. *J. Climate*, **9**, 270–304.
- Delworth, T. L., A. J. Broccoli, A. Rosati, R. J. Stouffer, V. Balaji, J. A. Beesley, W. F. Cooke, K. W. Dixon, J. Dunne, K. A. Dunne, J. W. Durachta, K. L. Findell, P. Ginoux, A. Gnanadesikan, C. T. Gordon, S. M. Griffies, R. Gudgel, M. J. Harrison, I. M. Held, R. S. Hemler, L. W. Horowitz, S. A. Klein, T. R. Knutson, P. J. Kushner, A. R. Langenhorst, H. C. Lee, S. J. Lin, J. Lu, S. L. Malyshev, P. C. D. Milly, V. Ramaswamy, J. Russell, M. D. Schwarzkopf, E. Shevliakova, J. J. Sirutis, M. J. Spelman, W. F. Stern, M. Winton, A. T. Wittenberg, B. Wyman, F. Zeng, and R. Zhang, 2006: GFDL's CM2 global coupled climate models - Part 1: Formulation and simulation characteristics. *J. Climate*, **19**, 643–674.
- Duffy, P. B., B. Govindasamy, J. P. Iorio, J. Milovich, K. R. Sperber, K. E. Taylor, M. F. Wehner, and S. L. Thompson, 2003: High-resolution simulations of global climate, part 1: present climate. *Clim. Dynam.*, **21**, 371–390.
- Hasumi, H. and S. Emori, 2004: K-1 Coupled GCM (MIROC) Description. Tech. Report No. 1, 2 pp. [Available from <http://www.ccsr.u-tokyo.ac.jp/kyosei/hasumi/MIROC/tech-repo.pdf>].
- Heideman, K. F. and J. M. Fritsch, 1988: Forcing mechanisms and other characteristics of significant summertime precipitation. *Wea. Forecasting*, **3**, 115–130.
- IPCC, 2000: *Special Report on Emissions Scenarios*. Cambridge University Press, Cambridge, UK, 432 pp.
- Le Treut, H. and Z. X. Li, 1991: Sensitivity of an atmospheric general circulation model to prescribed SST changes: feedback effects associated with the simulation of cloud optical properties. *Clim. Dynam.*, **5**, 175–187.
- Moorthi, S. and M. J. Suarez, 1992: Relaxed Arakawa-Schubert: A parameterization of moist convection for general circulation models. *Mon. Wea. Rev.*, **120**, 978–1002.
- Pan, D. M. and D. A. Randall, 1998: A cumulus parameterization with a prognostic closure. *Quart. J. Roy. Meteor. Soc.*, **124**, 949–981.
- Randall, D. A., T. A. Wood, S. Bony, R. Colman, T. Fiechter, J. Fyfe, V. Kattsov, A. Pitman, J. Shukla, J. Srinivasan, R. J. Stouffer, A. Sumi, and K. E. Taylor, 2007: Climate Models and Their Evaluation. *Climate Change 2007: The Physical Science Basis. Contribution of Working Group I to the Fourth Assessment Report of the Intergovernmental Panel on Climate Change*, Solomon, S., D. Qin, M. Manning, Z. Chen, M. Marquis, K. B. Averyt, M. Tignor, and H. L. Miller, Eds., Cambridge University Press, Cambridge, United Kingdom and New York, NY, USA.
- Rotstayn, L. D., 1997: A physically based scheme for the treatment of stratiform clouds and precipitation in large-scale models. I: Description and evaluation of microphysical processes. *Quart. J. Roy. Meteor. Soc.*, **123**, 1227–1282.
- Schmidt, G. A., R. Ruedy, J. E. Hansen, I. Aleinov, N. Bell, M. Bauer, S. Bauer, B. Cairns, V. Canuto, Y. Cheng, A. DelGenio, G. Faluvegi, A. D. Friend, T. M. Hall, Y. Hu, M. Kelley, N. Y. Kiang, D. Koch, A. A. Lacis, J. Lerner, K. K. Lo, R. L. Miller, L. Nazarenko, V. Oinas, J. Perlwitz, J. Perlwitz, D. Rind, A. Romanou, G. L. Russell, M. Sato, D. T. Shindell, P. H.

Stone, S. Sun, N. Tausnev, D. Thresher, and M. S. Yao, 2006: Present day atmospheric simulations using GISS ModelE: Comparison to in-situ, satellite, and reanalysis data. *J. Climate*, **19**, 153–192.

Sun, Y., S. Solomon, A. Dai, and R. W. Portmann, 2006: How often does it rain? *J. Climate*, **19**, 916–934.

Sundqvist, H., 1978: A parameterization scheme for nonconvective condensation including prediction of cloud water content. *Quart. J. Roy. Meteor. Soc.*, **104**, 677–690.

Sundqvist, H., E. Berge, and J. E. Kristjánsson, 1989: Condensation and cloud parameterization studies with a mesoscale numerical weather prediction model. *Mon. Wea. Rev.*, **117**, 1641–1657.

Tiedtke, M., 1993: Representation of clouds in large-scale models. *Mon. Wea. Rev.*, **121**, 3040–3061.

Xie, S., K. M. Xu, R. T. Cederwall, P. Bechtold, A. D. DelGenio, S. A. Klein, D. G. Cripe, S. J. Ghan, D.

Gregory, S. F. Iacobellis, S. K. Krueger, U. Lohmann, J. C. Petch, D. A. Randall, L. D. Rotstayn, R. C. J. Somerville, Y. C. Sud, K. V. Salzen, G. K. Walker, A. Wolf, J. J. Yio, G. J. Zhang, and M. Zhang, 2002: Intercomparison and evaluation of cumulus parameterizations under summertime midlatitude continental conditions. *Quart. J. Roy. Meteor. Soc.*, **128**, 1095–1135.

Zhang, G. J. and N. A. McFarlane, 1995: Sensitivity of climate simulations to the parameterization of cumulus convection in the Canadian Climate Centre general circulation model. *Atmos.-Ocean*, **33**, 407–446.

Zhang, M., W. Lin, C. S. Bretherton, J. J. Hack, and P. J. Rasch, 2003: A modified formulation of fractional stratiform condensation rate in the NCAR Community Atmospheric Model (CAM2). *J. Geophys. Res.*, **108**, doi:10.1029/2002JD002 523.

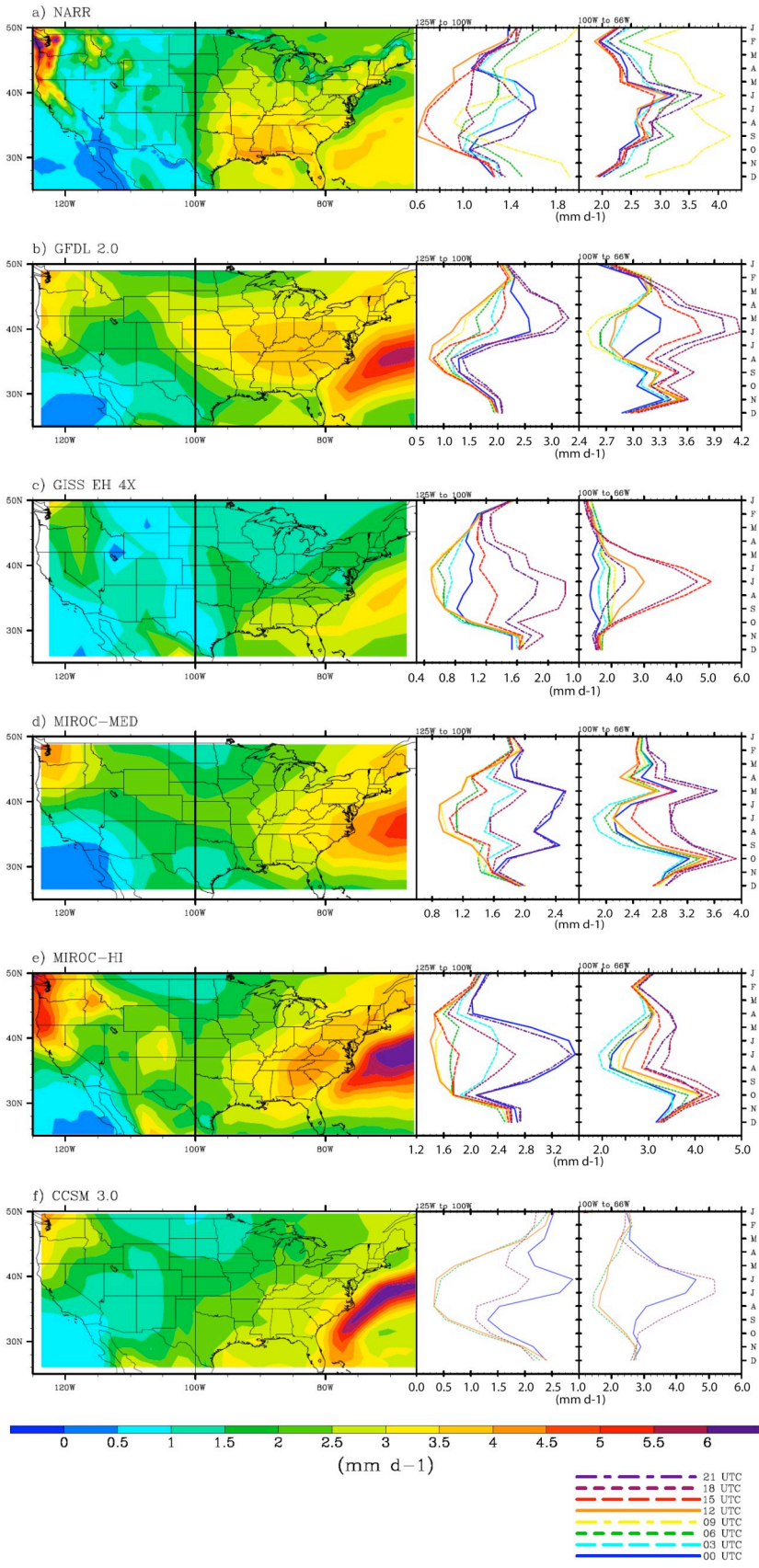


Fig. 1. 1991-2000 annual average precipitation rate (left column, mm/day, contours) and 3h monthly average precipitation rate for the domain shown in the left column from 125°W to 100°W (center column, mm/day) and from 100°W to 76°W (right column, mm/day) for: a) NARR, b) GFDL 2.0, c) GISS EH, d) MIROC-MED, e) MIROC-HI. Panel f): same, but for 1991-1999. and 6h monthly average precipitation rate from CCSM 3.0. The month of the year for the center and right columns is noted on the right-most y-axis by the first letter of each month. The divide between the two halves of the US at 100°W is indicated on the images in the left column by the heavy black line. Note: GISS EH precipitation was multiplied by a factor of four to facilitate comparison with the other models.

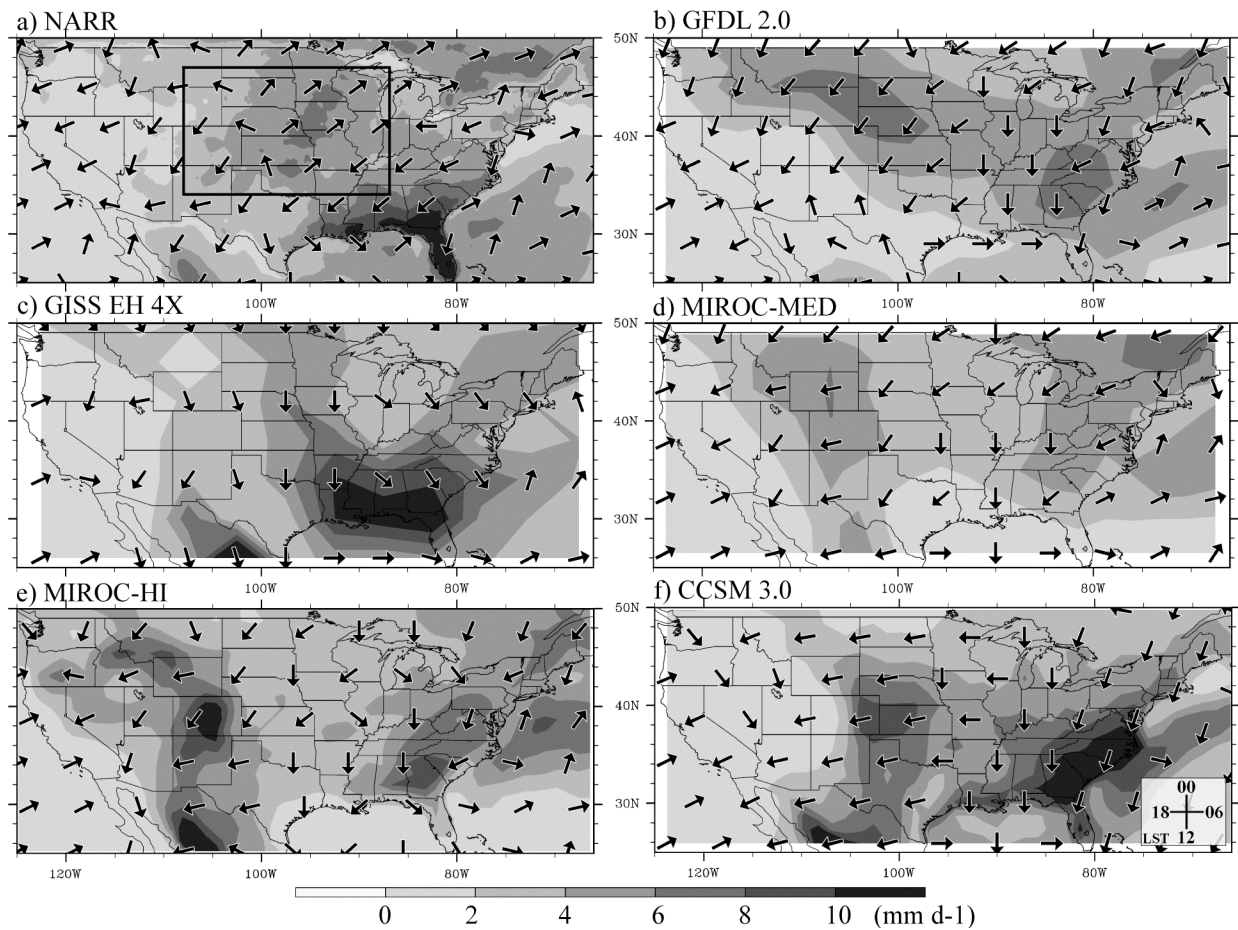


Fig. 2. 1991-2000 JJA maximum 3h average precipitation rate (mm/day, contours) and time of (vectors, LST) from a) NARR, b) GFDL 2.0, c) GISS-EH (precipitation multiplied by a factor of 4), d) MIROC-MED, e) MIROC-HI. Panel f): same, but for 1991-1999 6h average precipitation rate from CCSM 3.0. Vector time clock key inset in panel f.

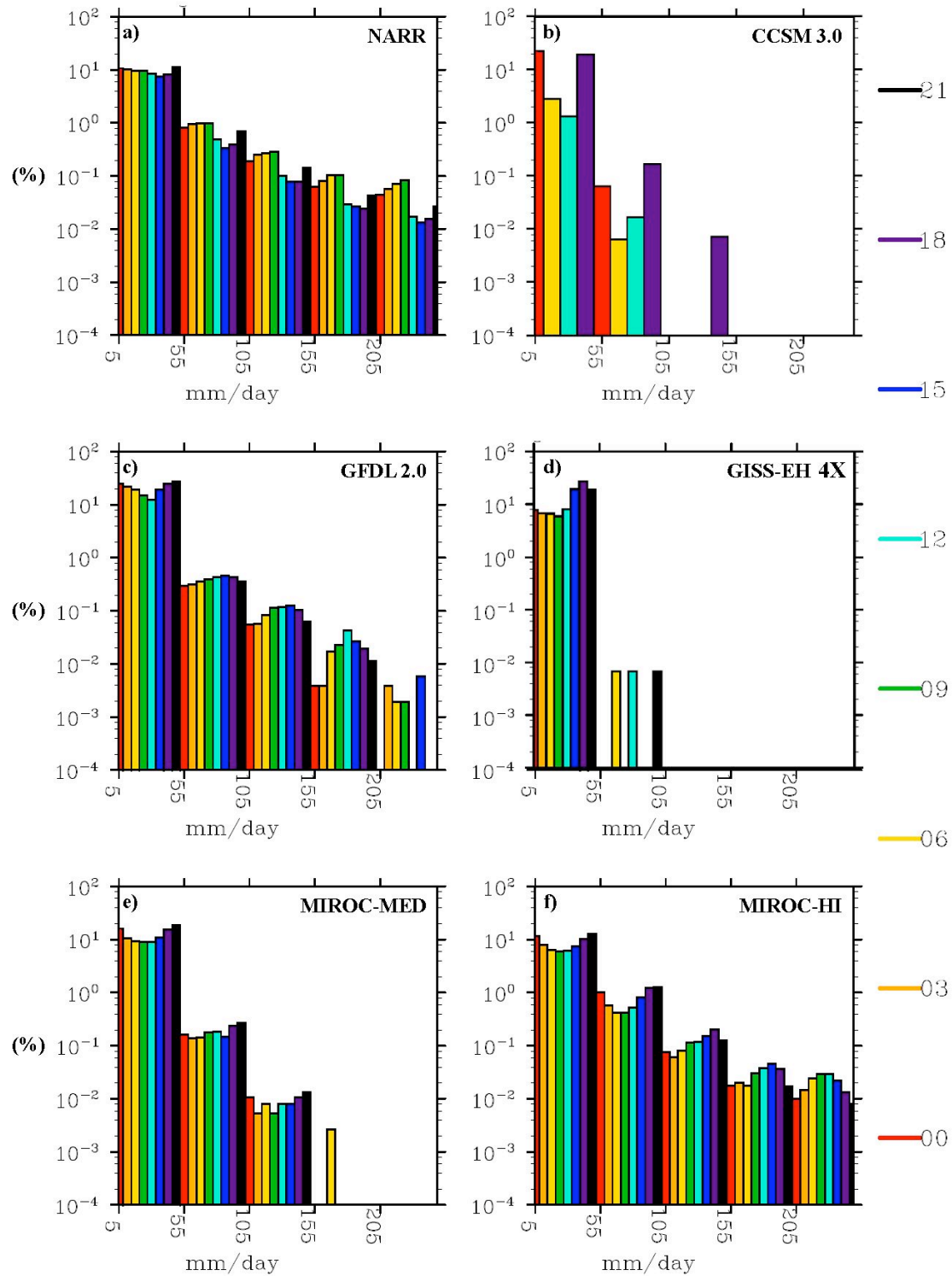


Fig. 3. 1991-2000 JJA 3h precipitation rate frequency distribution for the domain outlined in fig.: a) NARR, c) GFDL 2.0, d) GISS-EH, e) MIROC-MED, f) MIROC-HI. Panel b): same, but for 1991-1999 6h precipitation rate from CCSM 3.0. Values used to calculate the distribution in d) were multiplied by a factor of 3.

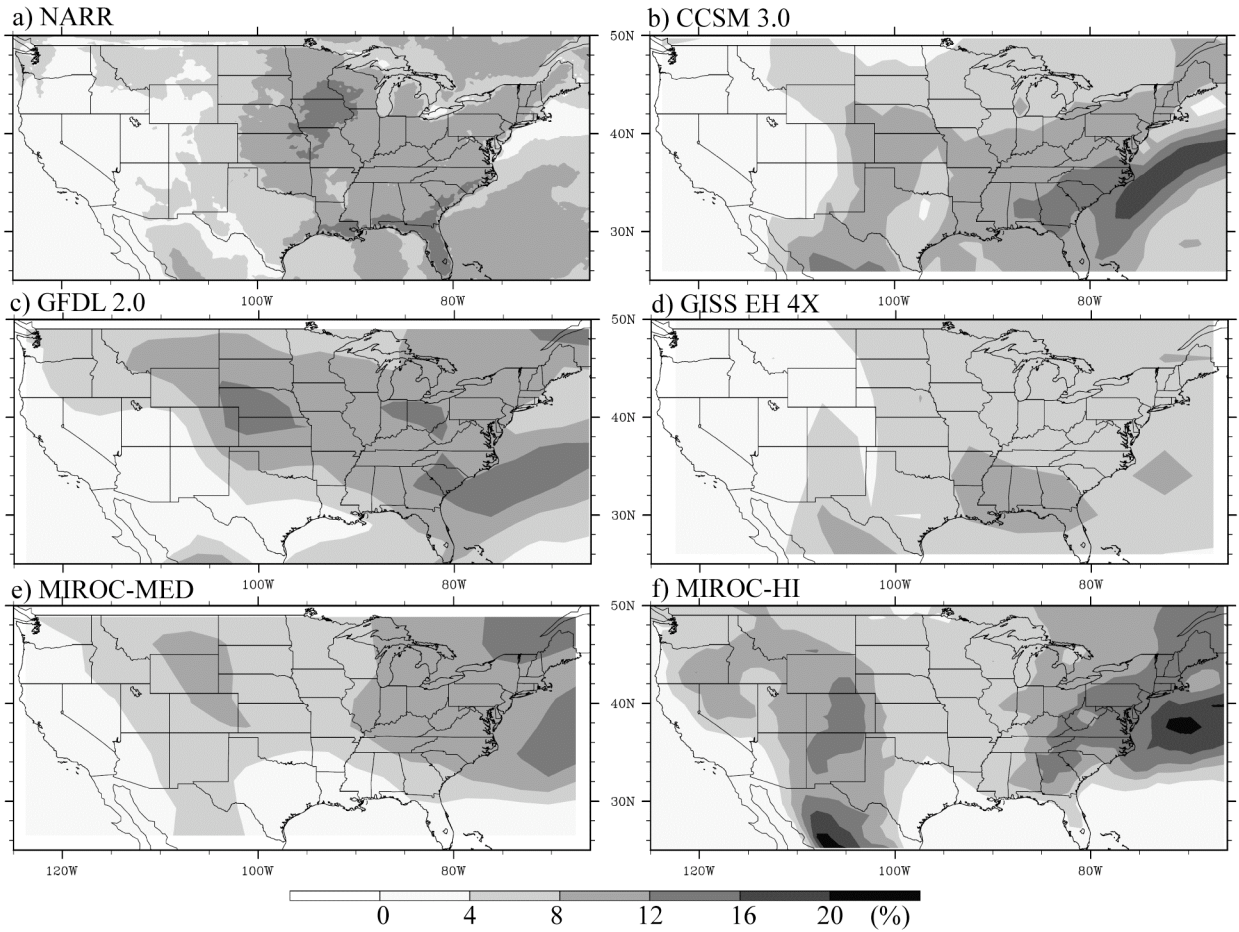


Fig. 4. 1991-2000 percent of the total daily precipitation in JJA greater than the JJA 90th percentile from: a) NARR, c) GFDL 2.0, d) GISS-EH, e) MIROC-MED, f) MIROC-HI. Panel b): same, but for 1991-1999 precipitation rate from CCSM 3.0. Values used in d) were multiplied by a factor of 4.

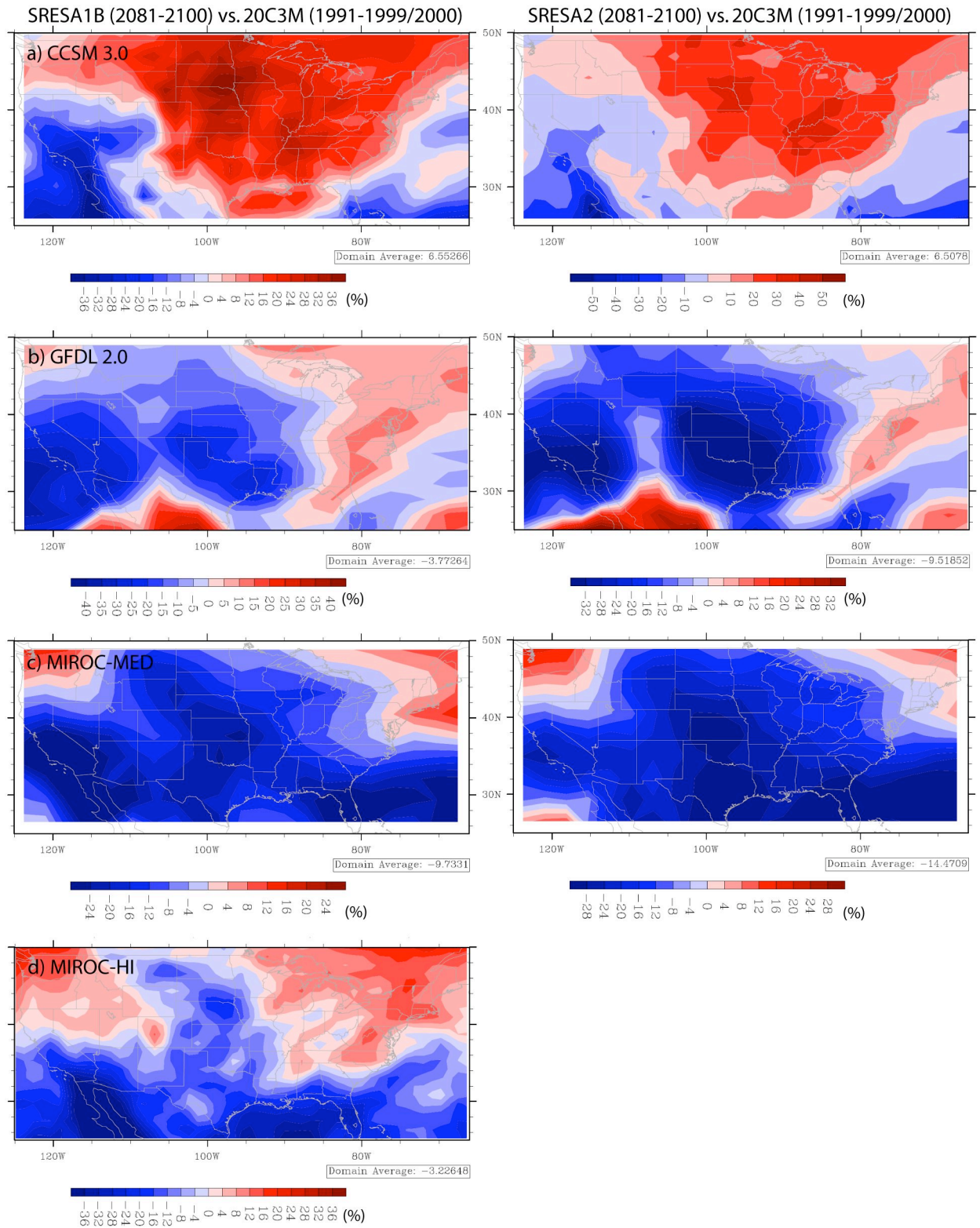


Fig. 5. Percent change in the annual mean between 1991-1999 and 2081-2100 for the SRESA1B (left column) and the SRESA2 scenario (right column) for a) CCSM 3.0. Panels b) GFDL 2.0, c) MIROC-MED, and d) MIROC-HI same, but for the percent change between 1991-2000 and 2081-2100.

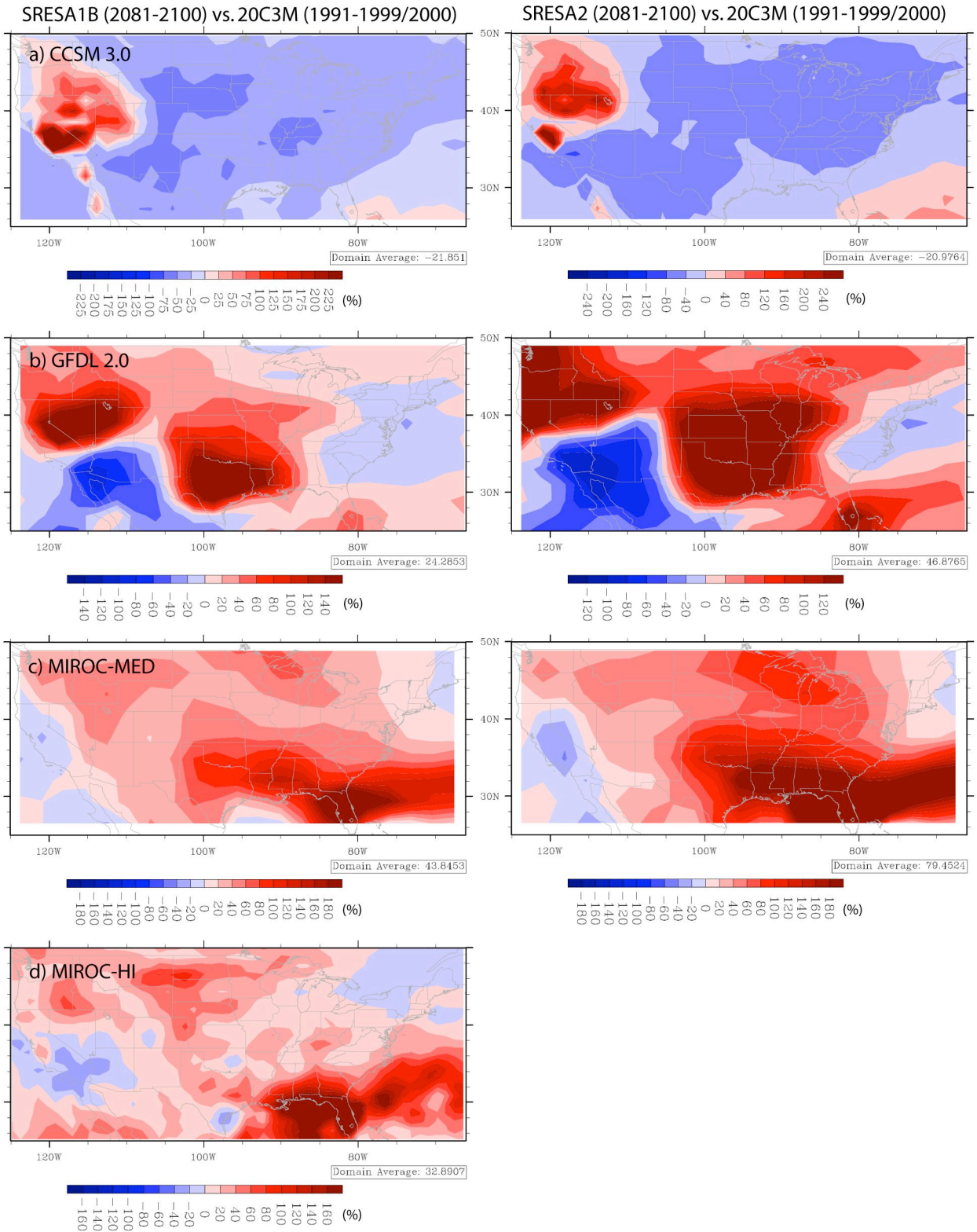


Fig. 6. Percent change in the percent of the total daily JJA precipitation greater than the 90th between 1991-1999 and 2081-2100 for the SRESA1B scenario (left column) and the SRESA2 scenario (right column) for a) CCSM 3.0. Panels b) GFDL 2.0, c) MIROC-MED, and d) MIROC-HI same, but for the percent change between 1991-2000 and 2081-2100.